



ELSEVIER

Contents lists available at [SciVerse ScienceDirect](http://www.sciencedirect.com)

## Biosensors and Bioelectronics

journal homepage: [www.elsevier.com/locate/bios](http://www.elsevier.com/locate/bios)

## Surface plasmon resonance detection of *E. coli* and methicillin-resistant *S. aureus* using bacteriophages

Nancy Tawil<sup>a,b,c,\*</sup>, Edward Sacher<sup>a</sup>, Rosemonde Mandeville<sup>b</sup>, Michel Meunier<sup>c</sup>

<sup>a</sup> Regroupement Québécois de Matériaux de Pointe, Département de Génie Physique, École Polytechnique de Montreal, Case Postale 6079, succursale. Centre-Ville, Montreal, Québec, Canada H3C 3A7

<sup>b</sup> Biophage Pharma Inc, 6100 Royalmount, Montreal, Québec, Canada H4P 2R2

<sup>c</sup> Laser Processing and Plasmonics Laboratory, Département de Génie Physique, École Polytechnique de Montreal, Case Postale 6079, succursale. Centre-Ville, Montreal, Québec, Canada H3C 3A7

## ARTICLE INFO

## Article history:

Received 2 March 2012

Received in revised form

11 April 2012

Accepted 13 April 2012

Available online 11 May 2012

## Keywords:

Bacteriophage

Biosensor

Methicillin-resistant *Staphylococcus aureus* (MRSA)

Surface plasmon resonance (SPR)

## ABSTRACT

Early diagnosis and appropriate treatment of *Escherichia coli* (*E. coli*) O157:H7 and methicillin-resistant *Staphylococcus aureus* (MRSA) are key elements in preventing resultant life-threatening illnesses, such as hemorrhagic colitis, hemolytic uremic syndrome, and septicemia. In this report, we describe the use of surface plasmon resonance (SPR) for the biodetection of pathogenic bacteria, using bacteriophages as the recognition elements. T4 bacteriophages were used to detect *E. coli*, while a novel, highly specific phage was used to detect MRSA. We found that the system permits label-free, real-time, specific, rapid and cost-effective detection of pathogens, for concentrations of  $10^3$  colony forming units/milliliter, in less than 20min. This system promises to become a diagnostic tool for bacteria that cause major public concern for food safety, bioterrorism, and nosocomial infections.

© 2012 Elsevier B.V. All rights reserved.

### 1. Introduction

Nosocomial infection is the leading cause of death for hospitalized patients, affecting more than 2 million such patients per year, and leading to approximately 90,000 deaths annually (Burke, 2003). The average treatment cost varies between \$14,000 and \$38,000 per patient, for a total reported cost of \$4.5 billion annually (Roberts et al., 2003). Methicillin-resistant *Staphylococcus aureus* (MRSA) is the leading cause of nosocomial and community-acquired infections. Reducing the time of diagnosis is directly related to reducing morbidity and mortality rates (Lindsey et al., 2008). A non-pathogenic form of *Escherichia coli* was used as a detection model for other harmful bacteria, such as *E. coli* O157:H7, a microorganism that causes severe gastrointestinal diseases in humans, such as bloody diarrhea, hemorrhagic colitis, and hemolytic uremic syndrome, reaching a mortality rate of over 50% in children and seniors (Easton, 1997).

Conventional culture methods that are predominantly used for bacterial detection are time-consuming and require enrichment steps in order to visualize colonies on agar plates. Over the years, mass spectrometry and biochemical detection systems have been

\* Corresponding author at: Département de Génie Physique, École Polytechnique de Montreal, Regroupement Québécois de Matériaux de Pointe, C.P. 6079, succ. Centre-ville, Montreal, Québec, Canada H3C 3A7.

E-mail address: [nancy.tawil@polymtl.ca](mailto:nancy.tawil@polymtl.ca) (N. Tawil).

developed to ameliorate and increase the speed and sensitivity of culture methods. However, these methods retain negative aspects such as high cost and difficulty in handling. PCR and immunoassays are other approaches aimed at ameliorating the sensitivity of detection. Nevertheless, routine PCR detects the presence of nucleic acid and cannot differentiate between live and dead cells. More importantly, PCR techniques still require DNA extractions, which are time-consuming and suffer from fidelity of DNA replication. In contrast, immunoassays, such as ELISA, are simple and rapid to use, but they lack suitable sensitivity for pathogen detection. Moreover, assay times vary from 24–52 h for bacteria (Kissinger 2005), which can be a decisive factor when treating a patient.

Other major shortcomings of the available biosensors are the use of ligands that cannot differentiate between pathogenic and non-pathogenic organisms with sufficiently high sensitivity and accuracy. Polyclonal antibodies recognize different epitopes on the same pathogens, which can also be present in related non-pathogenic organisms (Dover et al., 2009). Major disadvantages of monoclonal antibodies are their relative instability to environmental fluctuations, which can limit their long term storage and their field applicability. Furthermore, their production remains time-consuming and costly.

Bacteriophages are the main regulators of microbial balance on earth, as they total an estimated  $10^{32}$  entities (Kutter and Sulakvelidze, 2005). The many advantages of bacteriophages

make them an excellent method for the detection and identification of bacterial pathogens. Among these advantages are the specificity of the interaction of this type of virus with its target host cell, its lytic ability, and its capacity to multiply during the infection process. They are able to distinguish between live and dead cells, and they are robust, easy to produce, and cost-effective.

Requirements for pathogenic bacterial detection are rapidity, sensitivity, specificity and cost. Recently, many groups have been involved in developing bacteriophage-based sensors for bacterial detection (Balasubramanian et al., 2007; Gervais et al., 2007; Nanduri et al., 2007; Oh et al., 2004; Olsen et al., 2006). Balasubramanian et al. were able to identify *Staphylococcus aureus* with a detection limit of  $10^4$  colony forming units/milliliter (cfu/mL); however, detection suffered from the physical adsorption of phages onto the sensor surface (Balasubramanian et al., 2007). Moreover, the phages were not directed against methicillin-resistant strains of *S. aureus*. Oh et al. used self-assembled G protein to immobilize antibodies (Oh et al., 2004), a strategy that cannot be used to detect *S. aureus*. Our group has employed biotinylated T4 bacteriophages to detect *E. coli* (Gervais et al., 2007), but the genetic modification of all phages is not possible. Although much work has been done, a low cost, specific, sensitive optical method for detecting low concentrations of pathogens, in a few minutes, has not been established.

Our work consists, in part, of creating an accurate and sensitive biosensor for bacterial detection, with the potential for miniaturization. We use an already characterized impedometric sensor (PDS, Biophage Pharma) (Caron et al., 2006) to screen for the specificity of the bacteriophage to its target bacterium. Direct impedometric detection is limited by the facts that the medium utilized must be optimized for electrical measurements, and that not all microorganisms generate an adequate amount of ionized metabolites to allow for their detection.

These limitations can be overcome by the use of surface plasmon resonance (SPR). We suitably modified an SPR apparatus for bacterial detection. Multiple strategies were used to improve the immobilization of recognition elements on sensor surfaces including the physisorption of phages and the covalent immobilization of phages via L-cysteine, glutaraldehyde and self-assembled monolayers; an article in preparation contains a fuller discussion of the interaction of these molecules with gold than is given here, as well as the optimal method for phage immobilization. We have isolated and characterized a lytic bacteriophage that can specifically recognize methicillin-resistant strains of *S. aureus*. More importantly, we report on a rapid, specific and cost-effective method of detecting  $10^3$  cfu of bacteria per mL.

## 2. Materials and methods

### 2.1. Surface plasmon resonance

A schematic diagram of the instrument design is shown in Fig. 1. A superluminescent light-emitting diode (SLED), operating at 650 nm, was used as the light source. This allowed for a reduction in speckle patterning and interference fringes as SLEDs present low temporal coherence, related to their large spectral bandwidth. This translates in noise reduction, which allowed for better signal processing and better sensitivity. An achromatic lens produced a collimated beam, which passed through a polarizer. The linear *p*-polarized light was then focalized by a lens, and excited surface plasmons on the sensing surface, situated on top of a coupling prism.

A commercial sensing surface (Platypus technologies), consisting in a microscope glass slide (BK7) covered by an adhesion layer

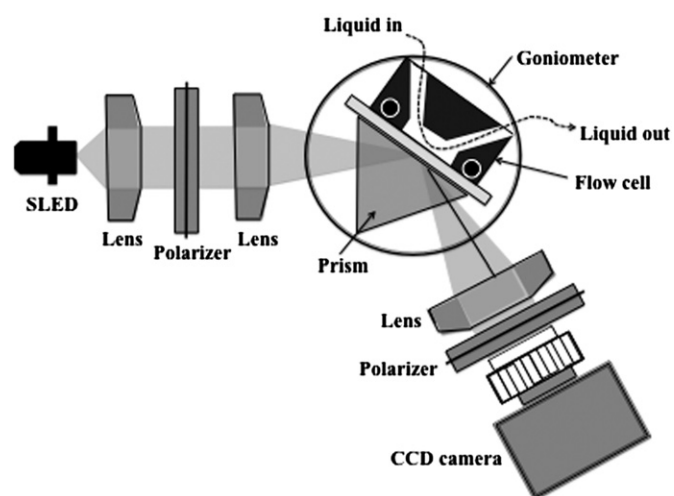


Fig. 1. Experimental CCD camera-based SPR set-up.

of 5 nm of titanium and a sensing layer of 50 nm of gold, was placed in oil immersion contact (Cargille Labs) on the top of the coupling prism (BK7 glass). For the real-time tests, a flow injection double channel-measuring cell, with 12  $\mu$ L volumes, was developed. The entire system was placed on a goniometer stage with 2-D linear translation for exact beam angle and beam position, permitting surface plasmon excitation on the gold/adjacent medium interface.

The spatial distribution of the reflected light intensity was recorded by a CCD camera (Hamamatsu C4742-95), and examined by appropriate software image treatment. The SPR resonance dip is usually recorded with a linear CCD detector. In our case, a drastic reduction of both signal noise and dispersion, which are due to the non-ideality of the light beam and the sensor surface modification, was achieved by using numerical analysis of the acquired SPR curves. Both fourth order polynomial curve fitting and centroid method were used to determine accurately the position of the SPR minimum.

Prior to SPR use, the gold surfaces of the glass slides were cleaned, using freshly prepared "piranha" solution (caution: piranha solution is a 3:1 mixture of concentrated  $H_2SO_4$  and 30%  $H_2O_2$ ), at room temperature, for 2 min, then rinsed thoroughly using MilliQ water, and dried in a nitrogen flow. The liquid flow rate ( $111 \mu\text{L min}^{-1}$ ) was controlled by a peristaltic pump (Ismatec). Phages specific for the targeted bacteria were then attached to the gold surface of the planar SPR system.

### 2.2. Impedance measurements

The impedance measurements were carried out using a PDS Biosensor (Biophage Pharma). The PDS biosensor is based on Electric Cell-Substrate Impedance Sensing (ECIS) and is used to detect the total live bacterial load of a sample. Small gold electrodes, 250  $\mu$ m in diameter, were placed on the bottom of individual culture wells. The sample, containing the bacteria and culture medium, was placed in the culture wells and a 4000 Hz, 1.5 V, 1  $\mu$ A current was applied between the detecting and the counter electrodes. The bacteria interfere with current flow as they occupy the free space immediately above the electrode; the impedance is monitored by a lock-in amplifier. Bacteriophages were immobilized on the gold electrode surface, following which, 400  $\mu$ L of freshly prepared bacterial solutions were injected into the well containing the gold sensor chip. The chip was then placed in an incubator at 37  $^\circ\text{C}$ . The growth of the bacteria was then monitored.

### 2.3. Chemicals

L-cysteine, 1-(3-imethylaminopropyl) ethylcarbodiimide hydrochloride (EDC), NHS, 11-mercaptoundecanoic acid, bovine serum albumin, sodium chloride, magnesium sulfate, and gelatin were purchased from Sigma-Aldrich. Luria-Bertani (LB) medium was purchased from Quelabs (Montréal, Québec, Canada); 25 g of LB powder were dissolved in 1 L of distilled water and autoclaved. LB-agar plates were prepared by adding 6 g of granulated agar to 400 mL of LB media. The LB-agar was autoclaved, melted and placed in Petri dishes. PBS was purchased from Fisher Scientific (Nepean, Ontario, Canada). *E. coli* K12 (11303) and T4 bacteriophages (11303-B4) were purchased from American Type Culture Collection (ATCC). SaA4 MRSA bacteria and BP14 bacteriophages were isolated by Biopharm.

### 2.4. Bacterial culture

EC12 and SaA4 bacteria were grown in an incubator-shaker at 37 °C in 4 mL of LB media for 3 h. The bacteria were then centrifuged at 2500 g (Sorvall RT7, 3500 rpm) for 20 min. The supernatant was discarded and the bacteria were resuspended in PBS. This was repeated twice. The concentration of bacteria was determined by plate count technique and expressed in colony forming units per milliliter (cfu/mL).

### 2.5. Bacteriophage preparation

Bacteriophages were amplified by pipetting 100 µL of a suspension of 10<sup>6</sup> pfu/mL of bacteriophages in a solution containing 1 mL of 10<sup>6</sup> cfu/mL of freshly prepared bacteria. After 15 min of incubation at room temperature, the infection mix was added to an Erlenmeyer flask containing 250 mL LB and incubated for 6 h, at 37 °C, in an incubator-shaker. The infected culture was then centrifuged at 2500 g for 20 min, then filtered (0.22 µm) and titrated. For the SPR measurements, the bacteriophages were further centrifuged for 60 min, the supernatant was removed and the phages were resuspended in PBS. The concentration of bacteriophages was determined by plate count technique and expressed in plaque forming units per milliliter (pfu/mL).

### 2.6. Optical density measurements

Bacterial suspensions were vortexed. One mL of the suspension was pipette in a disposable cuvette (Sarstedt AG & Co., Numbrecht, Germany). Optical density (OD) was monitored at 595 nm on a Beckman DU-140B spectrophotometer (Beckman Coulter Inc., Fullerton, CA).

### 2.7. Transmission electron microscopy

The TEM used was a Hitachi H-7100, operating at 75 kV. We used copper grids (200 mesh), coated with a layer of Formvar and an overlayer of evaporated amorphous carbon. The samples were deposited on the grid by the reverse drop method (a drop of sample was deposited on Parafilm for 5 min, then the grid was deposited on top of the Parafilm, and excess was wiped up with a paper towel). The grid was then dipped, for 1 min, in a drop of 3% aqueous phosphotungstic acid (PTA) adjusted to a pH of 7; PTA is a negative stain solution, used at neutral pH because phages will tend to dissociate at low pH. The grid was allowed to dry before the sample was used for TEM analysis.

### 2.8. DNA sequence analysis and bioinformatics

Open reading frame identification was performed using GeneMark.hmm (Lukashin and Borodovsky, 1998). Similarity searches, for nucleotide sequences and for the deduced amino acid sequences, were performed using the FASTA (Pearson, 1990), BLAST (Altschul et al., 1990), and PARALIGN (Rognes and Seeberg, 2000) programs available on the Online Analysis Tools website (<http://molbio-tools.ca/>).

## 3. Results and discussion

### 3.1. Specificity of BP14 for MRSA

To facilitate the immobilization and detection processes, bacteriophages should possess morphological characteristics, such as small size, and a short tail. For example, the T4 phage has a 168.9 kb genome, its head dimension is 110 × 80 nm, while its tail length 98 nm (Abuladze et al., 1994; Comeau et al., 2007). Because the evanescent wave of our SPR travels up to 300 nm into the substrate, only a portion of the bacterium will generate a response by interacting with it. Reducing the length of the recognition element will increase the SPR response on bacterial attachment. The transmission electron microscopic (Lustemberg et al., 2008) image of BP14 (Fig. 2a) shows its morphology to be very similar to that of the *S. aureus* 44AHDJ virus, allocated to the order *Caudovirales* and the family *Podoviridae*. It possesses a short, non-contractile tail measuring 25 nm (black arrow), and a small isometric head, measuring 42 nm (white arrow). It has a pre-neck appendage characteristic of the φ29-like phages, according to the International Committee on Taxonomy of Viruses. BP14 is 68% smaller than T4. This observation indicates that a larger portion of the target bacteria (~233 nm) can be probed by the evanescent field of the SPR, yielding an improved response (Fig. 2b).

The complete DNA sequence of BP14 was determined. The genome of BP14 consists of 17,769 base pairs (bp), and the total G+C content is 29.6%. Twenty-two open reading frames (ORFs) were identified, with 12 orientated in opposite directions from each other. The overall DNA sequence identity between BP14 and similar phages are 85.7% for Bacteriophage 66, 85.9% for *S. aureus* phage phiP68, 73% for *Staphylococcus* phage phi44AHJD, and 82% for *Staphylococcus* phage SAP-2. Of the 22 ORFs found, ORF-14 and 15 were identified as major and minor tail proteins, respectively, based on the overall similarity to tail proteins of the φ29 phage family. In particular, the sequence coding for the minor tail protein of BP14 differs from that of phage phiP68 by 11.2%, of *Staphylococcus* phage 66 by 9.8%, and of *Staphylococcus* phage SAP-2 by 63.7%. Our results suggest that phage BP14 is unique and different from other commercially available phages. Bacterial recognition is achieved by tailed-phages through the interaction of fibers at their tails. These fibers will first recognize, and adhere to, the host bacterium in a reversible fashion, followed by the irreversible binding of a secondary minor tail protein to another receptor molecule on the surface of the bacterium. Having a short, non-contractile tail, the phage has the advantage of not being able to fold and interact with the gold substrate on which it is deposited. Moreover, BP14 has a lesser probability of adhering to the gold surface by its tail, compared to phages with larger tail/head ratios.

Moreover, phages can be further divided into two categories, depending on their life cycles and means of propagation (Mandeville et al., 2003). BP14 is a member of the virulent phages, which are only capable of lytic propagation, consisting of infection of the host bacterium by the phage, replication of the phage genome, production of the phage structural components, and

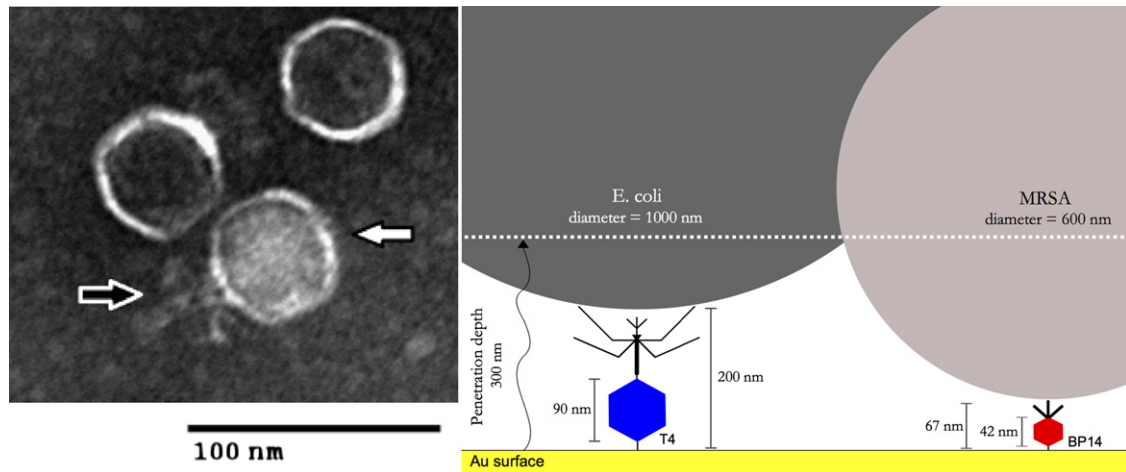


**Fig. 2.** (a) TEM image of bacteriophage BP14, showing an icosahedral head, measuring 42 nm in diameter (white arrow), and a 25 nm non-contractile tail (black arrow). (b) Comparison between T4 and BP14 bacteriophages. The use of a smaller bacteriophage, such as BP14, allows for a larger portion of the bacterium to be probed by the evanescent field.

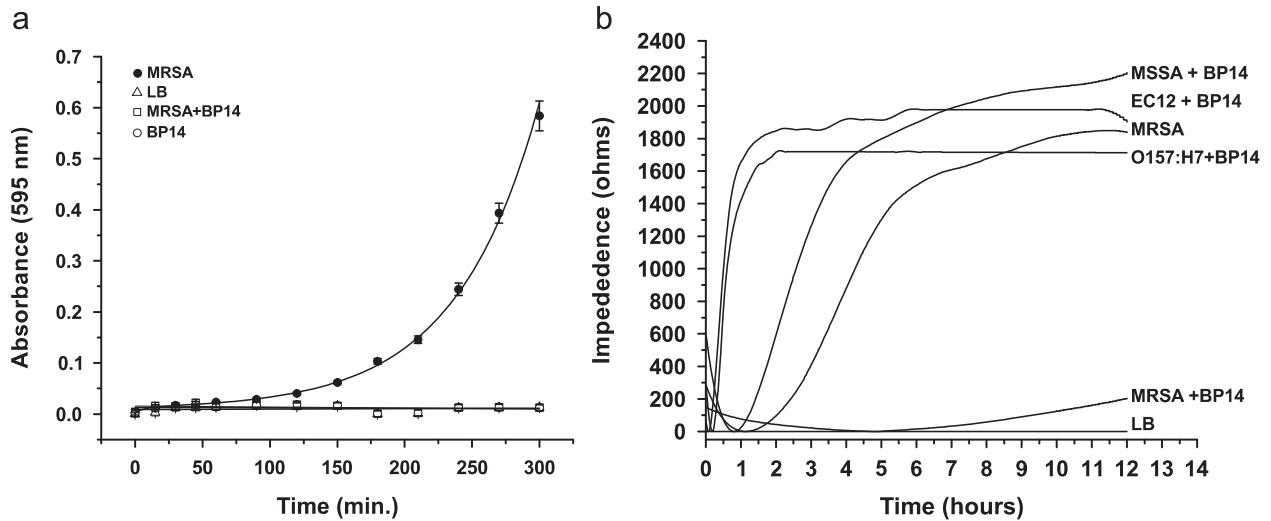


**Fig. 3.** Specificity of bacteriophage BP14 to MRSA bacteria. (a) Optical density of MRSA (positive control), LB (negative control), bacteriophage BP14, and MRSA and BP14 solution. (b) MRSA, MSSA, *E. coli* EC12 and O157:H7 were incubated with BP14 at 37 °C. Impedance was monitored for 12 h, reflecting bacterial growth. Replications of MSSA, EC12 and O157:H7 were not hindered by the presence of BP14. MRSA growth was delayed by the presence of BP14; MRSA bacteria are lysed following bacteriophage replication.

release of the newly assembled phages. More often than not, this process results in bacterial lysis and death. This is crucial for cost-effective production.

To establish whether bacteriophage BP14 possesses lytic capabilities, it was exposed to MRSA, and the optical density was monitored over time (Fig. 3a). We found that the optical density of BP14+MRSA did not increase over time, indicating that BP14 specifically recognizes MRSA, binds to the bacteria and lyses them, ultimately inhibiting their growth. Solutions containing only MRSA show an increase in optical density over time, consistent with bacterial growth.

In order to ensure the specificity of the sensor, the non-specific adsorption of entities other than the bacterium of interest must be prevented. Moreover, the selected phages should discriminate between MRSA and methicillin-sensitive *S. aureus* (MSSA), which is affected by the use of antibiotics. To demonstrate that BP14 can discriminate between different types of bacteria, we used an impedance biosensor to detect the total live bacterial load on a sensor chip. Bacteria act as insulating particles, by reducing the area that the current reaches and, thus, increasing the interface impedance. Because a bacteriophage specifically recognizes a host

bacterium and lyses it, the microbial growth will be reduced and, therefore, the detection time will increase in the wells containing the samples treated with phages. Here, the gold electrodes were first coated, using a solution of bovine serum albumin (BSA), to prevent non-specific binding. Following this, 400 µL of solution was pipetted into each cuvette and placed in an incubator at 37 °C for 12 h. The LB curve, in Fig. 3b, contains only culture medium and shows that there was no contamination present, while the MRSA curve contains only bacteria and shows their unhindered growth. Other wells contained bacteriophage BP14, incubated in the presence of various solutions of bacteria (EC12, O157:H7, MSSA, and MRSA), at a concentration ration of 1:5. Our results indicate that BP14 does not affect the growth of different *E. coli* strains, such as EC12 and O157:H7. Moreover, BP14 does not recognize, or lyse, methicillin-sensitive *S. aureus*. However, when in the presence of MRSA, BP14 provokes a delay in the growth of the bacterium. This observation signifies that BP14 is able to specifically recognize, adhere to, replicate, and lyse MRSA. The impedance decrease that can be observed in the first 30–60 min is due to the fact that bacteria release molecules to prepare their environment for growth. When bacteria grow in a culture

medium, they transform uncharged reactants, such as carbohydrates, into charged products, mainly carboxylic acids. These molecules render the culture medium more conductive, with a resultant decrease in impedance.

### 3.2. Detection of *E. coli* and MRSA

We used a home-built biosensor, with bacteriophages as specific recognition elements, to detect low concentrations of bacteria. Gold was coated with a self-assembled monolayer (SAM) of L-cysteine overnight at 37 °C, washed and subsequently coated with mercaptoundecanoic acid (MUA), then treated with 1-(3-dimethylaminopropyl)ethylcarbodiimide hydrochloride (EDC) and N-hydroxysuccinimide (NHS). A PBS solution was injected onto the SAM-modified gold chip for 10 min, followed by the injection of a PBS solution containing  $10^9$  pfu/mL phages for 50 min (Fig. 4). PBS was then injected to wash away the unbound phages, and  $10^6$  cfu/mL of the target bacterium was flowed over the sensor for 50 min, followed by washing. Because the lytic cycle of the phage is 30 min, we chose to follow the initial 20 min of surface plasmon response, following the injection of bacteria (dashed lines). The results are shown in pixels, with one pixel corresponding to 0.005 angle units.

To determine the sensor detection limit, we coated the gold chips with bacteriophage, using the previously described method. Furthermore, the chips were coated with BSA to prevent non-specific binding, followed by the injection of different concentrations of target bacteria. A solution of PBS was injected for the first 10 min, to create a baseline, after which a solution of *E. coli* in PBS was injected onto the sensor for another 20 min (Fig. 5). Bacteriophages will lyse the bacteria within 20 min following their attachment to their hosts. A significant change in the surface plasmon response can be seen after 10 min. The control consists of PBS injected onto a T4-coated gold chip.

The same experiment was repeated to establish the possibility of detecting MRSA bacteria, using BP14 combined with SPR (Fig. 6). All slides were previously coated with BP14 bacteriophages and BSA, to prevent non-specific adsorption. The controls consist of PBS injected onto a BP14-coated slide, and a solution of  $10^6$  cfu/mL of EC12 injected on a BP14-coated slide. Because EC12 are *E. coli* bacteria, and BP14 are not specific to this type of bacteria, we saw no significant change in SPR response. Noise was

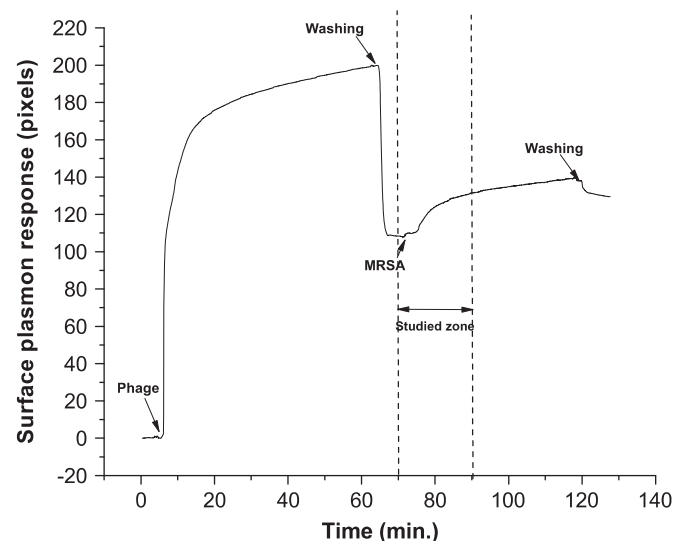


Fig. 4. SPR response of attachment of phages, followed by specific attachment of bacteria. The dashed lines indicate the region of interest for phage assisted detection.

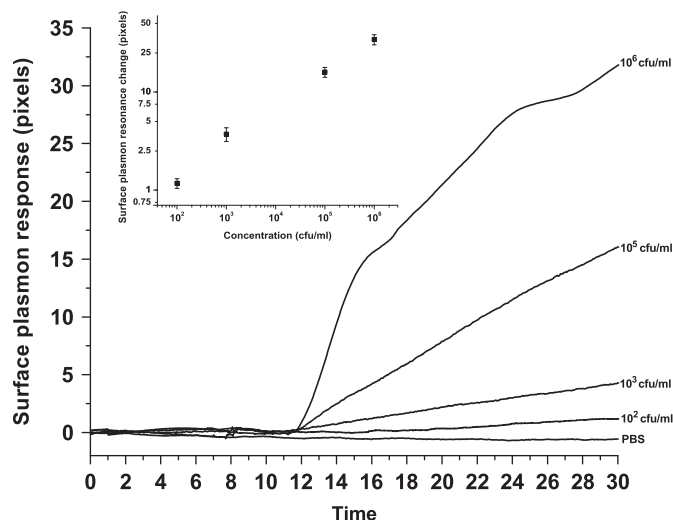


Fig. 5. Detection of *E. coli*, using T4 bacteriophages. T4 bacteriophages were coated onto the gold sensor chip. A baseline was created by injecting PBS buffer for 10 min. Following this, known concentrations of *E. coli*, diluted in PBS, were flowed over the sensor surface. The surface plasmon resonance change was monitored for 20 min. A dose-response curve for detection of *E. coli* is shown, in inset, for values taken after 20 min following bacterial insertion.

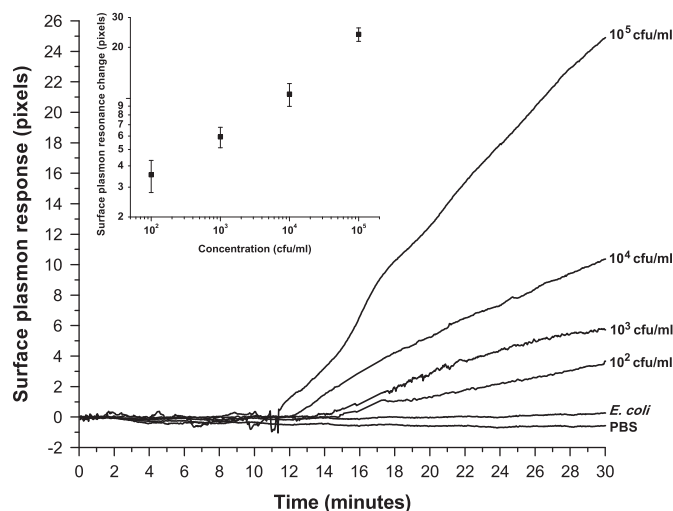


Fig. 6. Detection of MRSA using BP14 bacteriophages. BP14 bacteriophages were immobilized on the gold sensor chip. A baseline was created by injecting PBS buffer for 10 min. Following this, known concentrations of MRSA diluted in PBS were flowed onto the sensor surface. Surface plasmon resonance change was monitored for 20 min. *E. coli*, at a concentration of  $10^6$  cfu/mL, was also tested, and showed the high specificity of the B14 for MRSA detection. For detection of MRSA, a dose-response curve is shown, in inset, for values taken after 20 min.

determined to be the surface plasmon response difference between the PBS baseline and the non-specific adsorption of *E. coli* bacteria, corresponding to 0.835 pixels. Using the criterion of  $S/N > 3$ , the limit of detection is found to be  $10^3$  cfu/mL. Fig. 6 demonstrates that the SPR response due to bacterial detection by bacteriophages is dose-dependent. All experiments were carried out at room temperature; better results are anticipated at 37 °C.

Our results are consistent with those reported by other groups (Balasubramanian et al., 2007; Singh et al., 2010). The interaction between the phage and the bacterium receptor is a reversible process, which is ultimately followed by irreversible binding, coinciding with the initiation of phage DNA translocation into the bacterium. These two steps are characterized by rapid and slow exponential relaxations (Moldovan et al., 2007). Given the

geometrical parameters of the phage and the bacterium, the rate of adsorption of phage binding can exceed the theoretical limit of adsorption determined by diffusion models (Moldovan et al., 2007). Moreover, despite the small size of the bacterial receptors and the fact that they are sparingly found on the bacterium wall, phage capture of the bacterium occurs on each collision.

#### 4. Conclusions

Using SPR, we have demonstrated the use of T4 bacteriophage to detect *E. coli*, as well as the use of BP14 to detect MRSA. Our work reveals the specificity of bacteriophage BP14 for MRSA bacteria, as none of the other strains of bacteria examined show any interaction with BP14, which targets MRSA and interferes with its replication. It was possible to detect concentrations of  $10^3$  cfu/mL, without prior labeling or enrichment steps, in less than 20 min. This method of detection is of interest not only for public health, but for other phages, which can be used to identify and target other types of bacteria, such as anthrax for bioterrorism prevention, and *E. coli* O157:H7 for the food and water industries.

#### Acknowledgments

We thank NanoQuébec for their financial support, R. Allain (INRS-Institut Armand Frappier, Montréal) for TEM assistance, V. Latendresse for art work on Fig. 2b, and M. Maisonneuve and S. Patskovsky for SPR assistance.

#### References

- Abuladze, N.K., Gingery, M., Tsai, J., Eiserling, F.A., 1994. *Virology* 199, 301–310.
- Altschul, S.F., Gish, W., Miller, W., Myers, E.W., Lipman, D.J., 1990. *Journal of Molecular Biology* 215, 403–410.
- Balasuubramanian, S., Sorokulova, I.B., Vodyanoy, V.J., Simonian, A.L., 2007. *Biosensors and Bioelectronics* 22, 948–955.
- Burke, J.P., 2003. *New England Journal of Medicine* 348, 651–656.
- Caron, E., Luong, J.H.T., Male, K.B., Mandeville, R., Mazza, A., Male, K., 2006. WO2005088287-A1; US2005208592-A1; EP1728069-A1. Nat Res Council Canada (Canada).
- Comeau, A.M., Bertrand, C., Letarov, A., Tétart, F., Krisch, H.M., 2007. *Virology* 362, 384–396.
- Dover, J.E., Hwang, G.M., Mullen, E.H., Prorok, B.C., Suh, S.-J., 2009. *Journal of Microbiological Methods* 78, 10–19.
- Easton, L., 1997. *British Journal of Biomedical Science* 54, 57–64.
- Gervais, L., Gel, M., Allain, B., Tolba, M., Brovko, L., Zourob, M., Mandeville, R., Griffiths, M., Evoy, S., 2007. *Sensors and Actuators B* 125, 615–621.
- Kissinger, P.T., 2005. *Biosensors and Bioelectronics* 20, 2512–2516.
- Kutter, E., Sulakvelidze, A., 2005. CRC Press, Boca Raton, Florida.
- Lindsey, W.C., Woodruff, E.S., Weed, D., Ward, D.C., Jenison, R.D., 2008. *Diagnostic Microbiology and Infectious Disease* 61, 273–279.
- Lukashin, A.V., Borodovsky, M., 1998. *Nucleic Acids Research* 26, 1107–1115.
- Lustemberg, P.G., Vericat, C., Benitez, G.A., Vela, M.E., Tognalli, N., Fainstein, A., Martiarena, M.L., Salvarezza, R.C., 2008. *Journal of Physical Chemistry C* 112, 11394–11402.
- Mandeville, R., Griffiths, M., Goodridge, L., McIntyre, L., Henchuk, T.T., 2003. *Analytical Letters* 36, 3241–3259.
- Moldovan, R., Chapman-McQuiston, E., Wu, X.L., 2007. *Biophysical Journal* 93, 303–315.
- Nanduri, V., Sorokulova, I.B., Samoylov, A.M., Simonian, A.L., Petrenko, V.A., Vodyanoy, V., 2007. *Biosensors and Bioelectronics* 22, 986–992.
- Oh, B.K., Lee, W., Kim, Y.K., Lee, W.H., Choi, J.W., 2004. *Journal of Biotechnology* 111, 1–8.
- Olsen, E.V., Sorokulova, I.B., Petrenko, V.A., Chen, I.H., Barbaree, J.M., Vodyanoy, V.J., 2006. *Biosensors and Bioelectronics* 21, 1434–1442.
- Pearson, W.R., 1990. *Methods in Enzymology* 183, 63–98.
- Roberts, R.R., Scott, R.D., Cordell, R., Solomon, S.L., Steele, L., Kampe, L.M., Trick, W.E., Weinstein, R.A., 2003. *Clinical Infectious Diseases* 36, 1424–1432.
- Rognes, T., Seeberg, E., 2000. *Bioinformatics* 16, 699–706.
- Singh, A., Arya, S.K., Glass, N., Hanifi-Moghaddam, P., Naidoo, R., Szymanski, C.M., Tanha, J., Evoy, S., 2010. *Biosensors and Bioelectronics* 26, 131–138.